Dynamic Range of the SKA images

Maxim Voronkov, Mark Wieringa

CSIRO ATNF

Abstract

We present a study of the dynamic range which can be reached for images produced with the SKA. Results of simulations carried out for one spiral layout (SKA concept description, June 2002) have shown that AIPS++ Clark CLEAN provides a dynamic range decreasing rapidly with the distance from the phase-tracking centre. Presumably, the most severe effect on the dynamic range is due to gridding and aliasing at the imaging stage. The Cotton-Schwab CLEAN where the model subtraction is performed in the visibility domain gives a constant dynamic range of about 10^8 or higher if one takes into consideration w-term in the relation between the sky brightness and visibilities while forming the model.

1 Introduction

High dynamic range is an important requirement for the SKA, a new generation radio telescope. Having a wide field of view and operating at relatively low frequencies this instrument should be able to detect a weak source in the presence of a number of strong sources. The problem of dynamic range is mostly a software problem. Therefore, the analysis of algorithms used to synthesize interferometric images becomes vital. This report contains new results of the follow-up study which deepens the previous simulation work by Voronkov & Wieringa (2003, hereafter Report I).

2 Simulations

All simulations were done in the same way as in the Report I. The study comprises the following two parts

1. Study of the Cotton-Schwab clean performance in the sense of off-axis dynamic range. A model was a point source away from the phase centre (like models in the Report I). Simulated observations were a pure snap-shot of one integration per baseline.

2. Dynamic range in a dirty image (i.e. without any deconvolution algorithm) for the case of long observation of a point source at the phase centre.

The first part was done using the Swinburne cluster. Each node of the cluster was assigned a separate AIPS++ job which includes a visibility prediction for a given offset of the point source from the phase centre, Cotton-Schwab clean (an implementation described in the Report I taking into account the w-term) and image analysis. Thus, the time required to calculate the whole dynamic range vs. offset plot was considerably reduced. The main goal of simulations in this part was to determine the dynamic range of the Cotton-Schwab clean in the presence of bandwidth smearing. In this case the interferometer responce to the point source away from the centre is no longer a point source convolved with a dirty beam. In the dirty image the response will have an elongated shape. This will create difficulties for the deconvolution algorithm and may limit the dynamic range. The SKA correlator should cope with spectral line data and, hence, bandwidth smearing should not be a serious problem in a real experiment because the total bandwidth could be split into a number of channels. However, an estimate of dynamic range loss in this case may be useful for further study of the algorithm. More important application of these simulations is a model when the point source is situated between image pixels. A decrease of dynamic range is a well known fact in this case (see e.g. Briggs, 1995). If there is only one strong source in the field, the image grid can be adjusted to have that source in the centre of the image cell. However, with 3 or more strong sources this is no longer possible. The SKA will need to deal with a large number of strong sources due to the wide field of view.

The second part of the study is related to imaging without deconvolution. Any deconvolution algorithm is difficult to analyze because analytical methods are often impractical. For some tasks it might be better not to use deconvolution at all. For long observations a spiral configuration of the SKA produces almost complete uv-coverage (of course bounded by array size). By using uniform weighting and appropriate tapering, it should be possible to create a synthesized beam without sidelobes. The cluster was not used for this part of the simulations due to the extreme disk space requirements (hundreds of GBytes).

3 Precision: doubles vs. floats

It became clear in the earliest stages of simulation that the AIPS++ visibility simulator is rather slow for large datasets. In addition, all models studied so far were very simple (basically a few point sources). We decided to implement our own code to predict

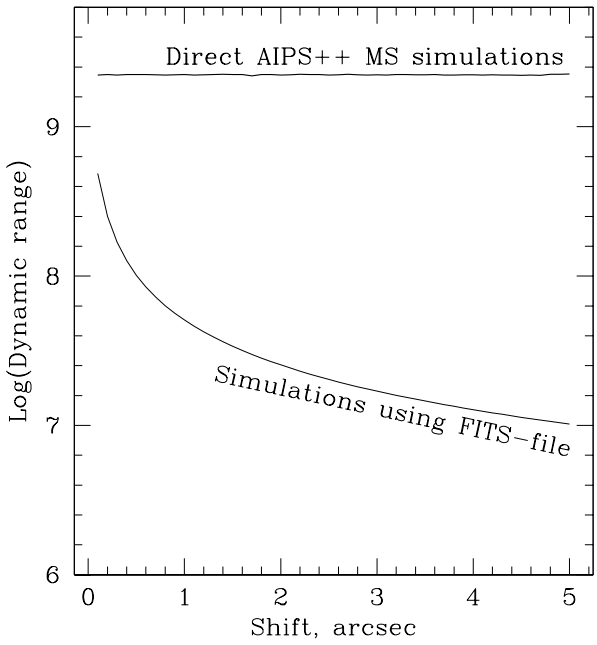

Figure 1: Dynamic range versus the source offset from the phase centre when u,v and w are stored as doubles (Direct AIPS++ Measurement Set writing) and as floats (FITS file).

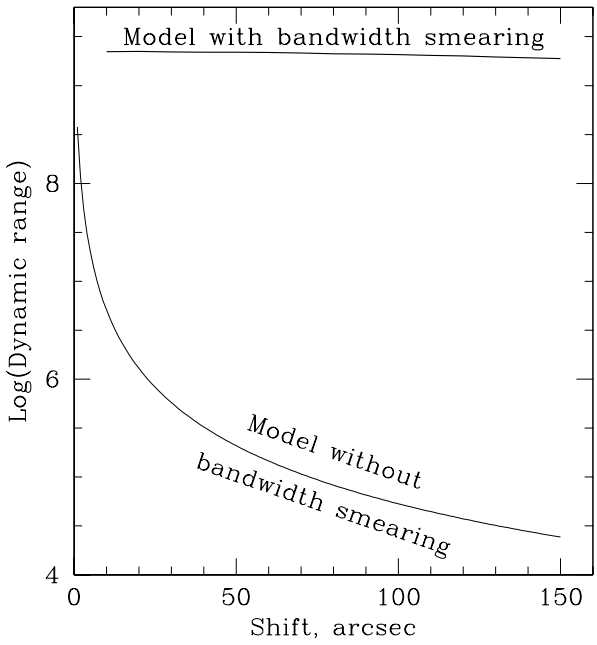

Figure 2: Dynamic range versus the source offset from the phase centre when the visibilities corresponding to each clean component were modeled along with the bandwidth smearing and without it.

visibilities. The first version of the code wrote a FITS file using the **cfitsio** library. Then, this FITS file was loaded into AIPS++ measurement set. The dynamic range decreases when the source offset from the phase centre increases (see Fig.1). The image has been deconvolved using the Cotton-Schwab clean algorithm with w-term, for which we obtained almost constant dynamic range in previous experiments with the AIPS++ visibility simulator (Report I). The difference between the two measurement sets created using the AIPS++ visibility simulator and the external code making use of the cfitsio library is in the floating point precision of the stored baseline spacings u,v and w. The AIPS++ visibility simulator calculates baseline coordinates with a double precision and then the visibility data were calculated from the source model and stored as single precision numbers. In contrast to this, due to limitations of the cfitsio library, u, v and w have the same precision as the visibility data. As a result, baseline spacings were stored with a rounding off error due to double to float conversion. A second version of the simulation code writes an AIPS++ measurement set directly avoiding FITS files and the usage of the cfitsio library. The dynamic range was constant if the data were simulated by the latter code (which preserves the precision of u,v and w,

see Fig.1). This fact means that at least baseline coordinates should be stored as a double precision floating point numbers to achieve a required dynamic range of about $10^6 - 10^7$.

4 Bandwidth smearing

Radio interferometers suffer from chromatic aberration (e.g., Thompson, et al. 1986). A spatial scale filtered by a baseline at a given time depends on the wavelength. In practice, interferometers have a finite bandwidth and, so different parts of the bandpass probe different spatial scales. This may lead to decorrelation of the signal and to image distortion if the bandwidth is wide. Of course, the further the source is from the centre, the more severe the effect is. If the deconvolution algorithm does not model the bandwidth smearing, it will degrade the dynamic range (see Fig.2). The simulations show that the reponse on the bandwidth smeared point source can not be well represented by a sum of responses without bandwidth smearing (clean components). May be this problem is related to bad performance of the clean algorithm in the case of extended sources, as the distorted image is no longer an image of the point source in the presence of the bandwidth smearing. Interestingly, if the bandwidth smearing is also modeled when the model visibilities are calculated from the set of clean components, the dynamic range is almost constant throughout the image (Fig. 2). In these simulations, the bandwidth was assumed to be unrealistically wide (256 kHz) to emphasize the effect. The SKA correlator will split the bandwidth into a number of spectral channels and the smearing will be much smaller. But even for such a wide bandwidth, an appropriate change of the software allows us to eliminate the impact of the bandwidth smearing on the dynamic range. From this we can conclude that the bandwidth smearing will not be a problem for the SKA in the sense of dynamic range.

5 Point source between pixels

For all previous simulations the source offset from the phase centre was an integral multiple of the cell size. If the offset is a fractional number the dynamic range decreases dramatically (see Fig.3). This effect is known and described e.g. by Briggs (1995). If there is only one strong source in the field of view it is always possible to adjust the grid to place that source on the centre of the grid cell. Unfortunately, this is not a solution for the SKA, whose images will contain a large number of strong sources. The effect originates from the discrete nature of the Fourier transform and

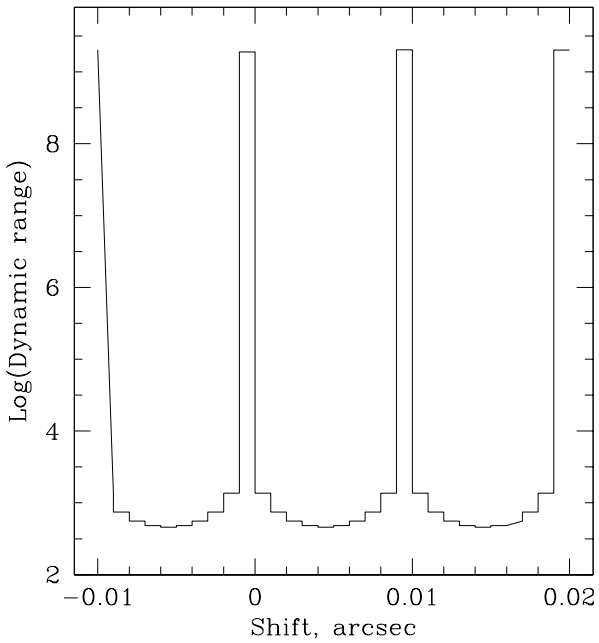

Figure 3: Dynamic range versus the source offset from the phase centre. Offsets are generally not integral multiples of the cell size (0.″01).

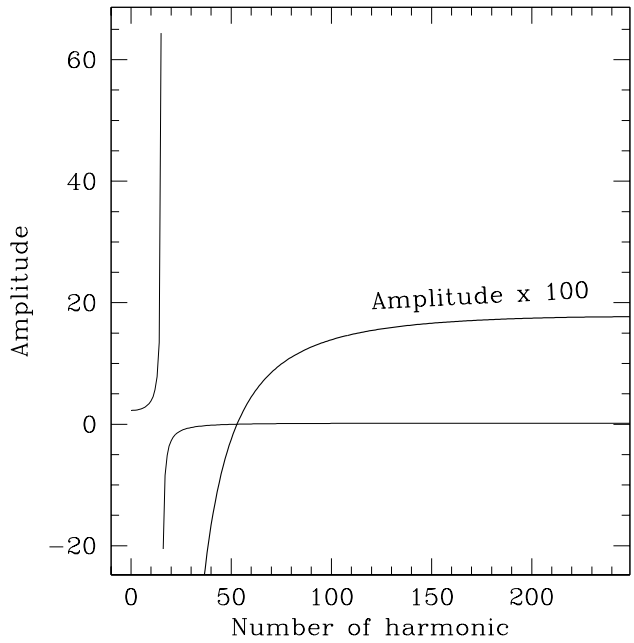

Figure 4: An FFT spectrum of the cosine function of some amplitude sampled at a fractional rate.

occurs regardless of whether the Fast Fourier or Direct Fourier transform is used. The discrete Fourier transform implies that the function to be transformed is periodic, with an integral multiple of the period being equal to the sample size. If the function is not periodic, the transform will not be equal to the original function but will correspond to a piecewise function with a discontinuity at the edges of the sampled interval (Gibbs phenomenon). A result of the Fast Fourier transform taken from the cosine function sampled at a fractional rate is shown in Fig.4. Here the following function

$$x_n = 100 \cos\left(\frac{30.5\pi n}{512}\right) \tag{1}$$

was sampled so n runs from 0 to 511. It can be seen that all harmonics are necessary to represent the cosine function with a fractional frequency. In terms of the 2-D Fourier transform and interferometric images this will decrease the dynamic range of the image. Further study of this effect is needed. Probably, other set of basis functions (not sine and cosine) could be used to form an image. For example, one can try to discretize the Fourier integral assuming the basis functions to be zero outside the sampled interval instead of being periodic. Because the cell size is a fraction of the synthesized beam size it is not important for most science to know the position of the source with a

Table 1: The dynamic range in the dirty image for long observations

Duration hour	log(Dynamic range)	Model
0.5	3.92	no taper, 400 channels of 5 MHz
1	4.19	no taper, 200 channels of 10 MHz
3	3.89	no taper, 100 channels of 20 MHz
3	2.54	taper $0''.05$, 100 channels of 20 MHz

precision better than the cell size. Thus, this feature of the discrete Fourier transform is just a technical impediment. Other algorithms and/or smaller cell size could alleviate the problem. Further simulations are necessary to understand how the strength of the effect depends on the cell size with the same synthesized beam.

6 Long observations

As it was stated before, in the case of very good uv-coverage, which could be achieved for long SKA observations (up to several hours) and bandwidth synthesis, the dynamic range might be high enough in the dirty image without any deconvolution. Appropriate tapering is required, however, to suppress the sidelobes arising from the cut off at large baselines. We carried out a set of simulations to find what dynamic range could be achieved using this approach. Because there was no deconvolution stage in these experiments, we could not use a residual image to calculate a dynamic range. Instead, the dynamic range was calculated as a ratio of the maximum in the dirty image to the rms noise calculated on the basis of all pixels outside a centered circle with a diameter equal to the half of the image size. Due to an extreme disk space requirements (sometimes up to 500 Gbytes) a few models were calculated only (see Table 1). All models contained no bandwidth smearing and simulated a point source at $\delta = -50^\circ$ at 8 GHz. It was possible to reach the dynamic ranges of about 10^4 in the models without taper. For still unexplained reasons, applying a taper makes the situation worse (see Table 1). This effect requires further study. It is worth to note that the dynamic range values are similar for all models shown in Table 1.

7 Conclusions

1. Floating point precision is a very important issue to reach a dynamic range of $10^6 - 10^7$. At least u,v and w should be stored as doubles.

2. Bandwidth smearing is not a problem (even for large channel bandwidth) if a model in the CS-clean takes it into account.

3. The highest dynamic range which was obtained in dirty images is 10^4. Tapering leads to a worse dynamic range.

4. The case of a source between pixels requires further study

References

Briggs D.S., High Fidelity Deconvolution of Moderately Resolved Sources, PhD thesis, The New Mexico Institute of Mining and Technology, Socorro, New Mexico, 1995

Thompson A.R., Moran J.M., Swenson G.W. Jr., Interferometry and Synthesis in Radio Astronomy, John Wiley & Sons, New York, 1986

Voronkov, M.A., Wieringa M.H., Study of Dynamic Range Limits of SKA Images (Report I), International SKA Conference, Geraldton, 27 July - 2 Aug, 2003 *http://astronomy.swin.edu.au/ska/SSWG/Meetings/Summary/Voronkov_Geraldton.ps*